

Analysis of laminated beams with a layer-wise constant shear theory

Julio F. Davalos,^a Youngchan Kim^a & Ever J. Barbero^b

^aDepartment of Civil Engineering, ^bDepartment of Mechanical and Aerospace Engineering, West Virginia University, Morgantown, West Virginia 26506-6101, USA

Based on generalized laminate plate theory, the formulation of a one-dimensional beam finite element with layer-wise constant shear (BLCS) is presented. The linear layer-wise representation of in-plane displacements permit accurate computation of normal stresses and transverse shear stresses on each layer for laminated beams with dissimilar ply stiffnesses. The BLCS formulation is equivalent to a first-order shear deformation beam theory (Timoshenko beam theory) on each layer. For the accurate computation of interlaminar shear stresses, the layer-wise constant shear stresses obtained from constitutive relations are transformed into parabolic shear stress distributions in a post-processing operation described in detail. The accuracy of the BLCS element is demonstrated by solving several numerical examples reported in the literature. While retaining the simplicity of a laminated beam theory, the element predicts results as accurate as much more complex elasticity analyses, and it is suitable to model frame-type structures.

1 INTRODUCTION

In Bernoulli-Euler (classical) and Timoshenko (first order shear deformation) beam theories, a plane section through the cross-section is assumed to remain plane after deformation. This assumption is sufficiently accurate for isotropic beams and for layered composite beams with plies of similar stiffnesses, but it leads to serious discrepancies with the actual state of stresses in laminated beams when one or more layers have quite different stiffnesses. To more accurately represent the actual response of isotropic or laminated beams, various explicit and numerical solutions have been proposed, as described next.

Rao and Ghosh¹ presented a plane stress elasticity solution of a laminated beam using Airy's stress function. Through a strength-of-materials approach, Levinson² included warping in such a way that satisfies the shear-free boundary conditions on the surfaces of the beam, obtaining a pair of coupled equations of motion. The theory could not, however, provide accurate results for a simply supported beam with uniform load. Rehfield and Murthy³ formulated a beam theory that includes the effects of transverse normal strain, transverse shear strain, and nonclassical axial stress with the help of a plane stress elasticity

solution of a simply supported beam under uniform load. However, the drawback of this theory is that the stresses, derived from a specific loading condition and from which strains are estimated, are not necessarily valid for an arbitrary loading condition. Including the transverse shear strain and nonclassical axial stress, Krishna Murthy⁴ formulated a beam theory in which a parabolic shear stress distribution across the depth of the beam is obtained from the constitutive equation.

A three-dimensional elasticity solution for symmetrically laminated rectangular beams is given by Cheng *et al.*,⁵ where each layer of the beam is assumed to be homogeneous, transversely isotropic, and unidirectionally reinforced. The explicit solution was found by using the equations of equilibrium and boundary conditions, and by determining the unknown coefficients in the assumed displacement and stress functions; a procedure known as the semi-inverse method (Timoshenko⁶). The solution was applied to a cantilever beam with a concentrated load at the tip and to a simply supported or clamped beam with a concentrated load at midspan.

Recent research has focused on the removal of the restriction of plane sections by introducing higher-order terms (mainly third-order) in the

kinematical description of the displacement field (Reddy⁷); an approach known as higher-order shear deformation theory (HSDT). In HSDT, the shear stress distribution through the cross-section is non-linear, and therefore a shear correction factor is not needed in the constitutive equation. Reddy⁸ presented a generalized formulation of higher-order laminate plate theory (GLPT) which can be specialized to a number of particular theories, such as Reddy *et al.*⁹ Incorporating linear transverse normal strain and quadratic transverse shear strain through the thickness of a beam, Kant and Gupta¹⁰ developed a higher-order beam theory and implemented a C^0 finite element with four degrees of freedom per node; convergence was very slow with the two-node finite element. Assuming transverse incompressibility, Kant and Manjunath¹¹ developed a set of higher-order displacement models in which the longitudinal displacements through the thickness can be expressed with up to cubic functions. The models were implemented for a C^0 four-node, cubic finite element, where the interlaminar transverse normal and shear stresses were computed from stress equilibrium equations. Using a displacement function similar to that proposed by Levinson² and following Reddy⁷ for the derivation of equilibrium equations, Gordaninejad and Ghazavi¹² developed a laminated beam theory with a mixed finite element discretization; the theory includes a second derivative of transverse displacement in the strain component and requires C^1 -continuity, which is not computationally efficient. Yuan and Miller¹³ derived a five-node finite element with a total of 16 degrees of freedom (dof) under the assumption of a cubic variation of the in-plane displacement through the thickness. Based on this element, a laminated beam element of N layers with a total of $9N+7$ dof was later developed.¹⁴ Surana and Nguyen¹⁵ extended HSDT to arbitrarily curved two-dimensional beam elements; their formulation allowed a variable order of approximation (p -version) in the transverse direction, including transverse normal strain. A thorough discussion of shear deformation theories is presented by Noor and Burton¹⁶ and Kapania and Raciti.¹⁷

Computation of accurate inter- and intralaminar stresses are important, because these

stresses can cause delaminations and initiation of failures in the laminates. Based on force and moment equilibrium and the principle of minimum complementary energy, Kassapoglou and Lagace¹⁸ presented a method to compute the three-dimensional stress state in a symmetric laminate plate under uniaxial load. Lajczok¹⁹ applied a finite difference technique to the computation of the derivatives of strains and curvatures obtained from MSC/NASTRAN. The derivatives are substituted into the equilibrium equations, from which the interlaminar shear stresses are computed. Using equilibrium and compatibility of stresses and assuming a parabolic shear stress distribution through the thickness of each layer, Chaudhuri and Seide²⁰ presented a method to compute the interlaminar shear stresses for a quadratic laminated triangular element. Similarly, Reddy *et al.*,⁹ described a layer-wise computation of shear stresses for laminated plates by integrating the equilibrium equations and using the in-plane stresses obtained from the finite element solution.

In the present study, a 1-D laminated beam finite element with layer-wise constant shear (BLCS) is formulated based on GLPT. The formulation of BLCS is much simpler than that of a similar N -layer beam element developed by Yuan and Miller.²¹ The layer-wise representation of in-plane displacement in BLCS permits accurate computation of normal and shear stresses on each layer for laminated beams with dissimilar ply stiffnesses, and the model allows for discontinuity in strains at layer interfaces. Plane stress and transverse incompressibility on each layer is assumed. The in-plane displacements are assumed linear on each layer, and the transverse displacement is constant through the thickness. The layer-wise constant shear stresses obtained from constitutive relations are transformed into parabolic distributions, following an approach similar to that presented by Chaudhuri and Seide²⁰ and Reddy *et al.*⁹ The model can predict the linear elastic behavior of straight cross-ply laminated beams with rectangular cross-sections consisting of symmetric or asymmetric laminates. Various numerical examples are solved, and the results are compared with other solutions presented in the literature.

2 LAYER-WISE CONSTANT SHEAR BEAM THEORY

Assuming transverse incompressibility and layer-wise representation of in-plane displacement (Reddy *et al.*⁹), the displacements of a point in a laminated beam can be written as

$$u_1(x, z) = u(x) + U(x, z), \quad u_2(x, z) = w(x) \quad (1)$$

where u and w are, respectively, the longitudinal and transverse displacements of a point on the reference axis of the laminate, and $U(x, z)$ is a function whose value is zero on the reference axis of the beam (Fig. 1):

$$U(x, z=0) = 0 \quad (2)$$

The function $U(x, z)$ represents layer-wise in-plane displacements and is approximated by continuous known functions $\phi^j(z)$ and undetermined coefficients $U^j(x)$:

$$U(x, z) = \sum_{j=1}^n U^j(x) \phi^j(z) \quad (3)$$

where $\phi^j(z)$ are any continuous functions that satisfy the condition

$$\phi^j(0) = 0 \quad \text{for all } j = 1, 2, \dots, n$$

A finite element approximation of the in-plane displacement through the thickness can be obtained from eqn (3) using Lagrangian interpolation functions (see Barbero²²). In BLCS, a layer-wise linear representation of in-plane displacements is used. The constitutive equation for a lamina, obtained from the transformed stress-strain relation of an orthotropic lamina under the assumption of plane stress (x - y plane) and without the transverse normal component (Jones²³), can be written as

$$\begin{Bmatrix} \sigma_x \\ \sigma_y \\ \sigma_{xy} \\ \sigma_{yz} \\ \sigma_{xz} \end{Bmatrix} = \begin{bmatrix} \bar{Q}_{11} & \bar{Q}_{12} & \bar{Q}_{16} & 0 & 0 \\ \bar{Q}_{12} & \bar{Q}_{22} & \bar{Q}_{26} & 0 & 0 \\ \bar{Q}_{16} & \bar{Q}_{26} & \bar{Q}_{66} & 0 & 0 \\ 0 & 0 & 0 & \bar{Q}_{44} & \bar{Q}_{45} \\ 0 & 0 & 0 & \bar{Q}_{45} & \bar{Q}_{55} \end{bmatrix} \begin{Bmatrix} \varepsilon_x \\ \varepsilon_y \\ \gamma_{xy} \\ \gamma_{yz} \\ \gamma_{xz} \end{Bmatrix} \quad (4)$$

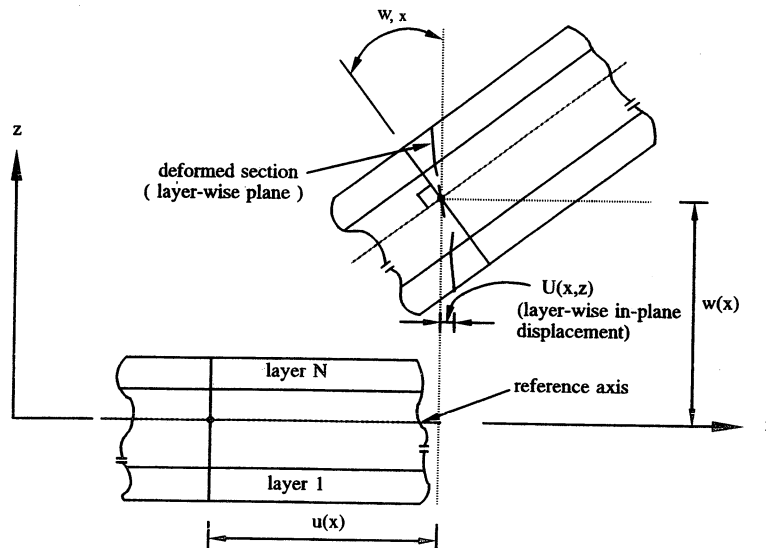


Fig. 1. Laminated beam geometry and displacement components.

In beam theory it is generally accepted that the following stresses are negligible: $\sigma_y = \sigma_{yz} = 0$. Furthermore, for a cross-ply lamina, $\sigma_{xy} = 0$. Imposing these conditions in eqn (4) and solving for the non-zero stress components, we obtain

$$\sigma_x = E_x \epsilon_x, \quad \sigma_{xz} = G_{xz} \gamma_{xz} \quad (5)$$

where

$$E_x = \bar{Q}_{11} + \bar{Q}_{12} \frac{\bar{Q}_{16} \bar{Q}_{26} - \bar{Q}_{12} \bar{Q}_{66}}{\bar{Q}_{22} \bar{Q}_{66} - \bar{Q}_{26} \bar{Q}_{26}} + \bar{Q}_{66} \frac{\bar{Q}_{12} \bar{Q}_{26} - \bar{Q}_{16} \bar{Q}_{22}}{\bar{Q}_{22} \bar{Q}_{66} - \bar{Q}_{26} \bar{Q}_{26}}, \quad G_{xz} = -\frac{\bar{Q}_{45}^2}{\bar{Q}_{44}} + \bar{Q}_{55}$$

Integrating σ_x and σ_{xz} in eqn (5) through the thickness of an N -layer laminated beam, the resultant forces can be derived as follows:

$$N_x = b \int_{-h/2}^{h/2} \sigma_x dz = b A_1 \frac{du}{dx} + b \sum_{j=1}^N B_1^j \frac{du^j}{dx} \quad (6a)$$

$$N_{xz} = b \int_{-h/2}^{h/2} \sigma_{xz} dz = b A_2 \frac{dw}{dx} + b \sum_{j=1}^N B_2^j u^j \quad (6b)$$

$$N_x^j = b \int_{-h/2}^{h/2} \sigma_x \phi^j dz = b B_1^j \frac{du}{dx} + b \sum_{j=1}^N D_1^{jj} \frac{du^j}{dx} \quad (6c)$$

$$N_{xz}^j = b \int_{-h/2}^{h/2} \sigma_{xz} \frac{d\phi^j}{dz} dz = b B_2^j \frac{dw}{dx} + b \sum_{j=1}^N D_2^{jj} u^j \quad (6d)$$

where b is the width of the beam. Expressed in matrix form, eqns (6) become,

$$\begin{Bmatrix} N_x \\ N_{xz} \end{Bmatrix} = b \begin{bmatrix} A_1 & 0 \\ 0 & A_2 \end{bmatrix} \begin{Bmatrix} \frac{du}{dx} \\ \frac{dw}{dx} \end{Bmatrix} + b \sum_{j=1}^N \begin{bmatrix} B_1^j & 0 \\ 0 & B_2^j \end{bmatrix} \begin{Bmatrix} \frac{du^j}{dx} \\ u^j \end{Bmatrix} \quad (7a)$$

$$\begin{Bmatrix} N_x^j \\ N_{xz}^j \end{Bmatrix} = b \begin{bmatrix} B_1^j & 0 \\ 0 & B_2^j \end{bmatrix} \begin{Bmatrix} \frac{du}{dx} \\ \frac{dw}{dx} \end{Bmatrix} + b \sum_{k=1}^N \begin{bmatrix} D_1^{jk} & 0 \\ 0 & D_2^{jk} \end{bmatrix} \begin{Bmatrix} \frac{du^k}{dx} \\ u^k \end{Bmatrix} \quad (7b)$$

where

$$A_1 = \sum_{k=1}^N \int_{z_k}^{z_{k+1}} E_x^{(k)} dz$$

$$A_2 = \sum_{k=1}^N \int_{z_k}^{z_{k+1}} G_{xz}^{(k)} dz$$

$$B_1^j = \sum_{k=1}^N \int_{z_k}^{z_{k+1}} E_x^{(k)} \phi^j(z) dz$$

$$B_2^j = \sum_{k=1}^N \int_{z_k}^{z_{k+1}} G_{xz}^{(k)} \frac{d\phi^j}{dz} dz$$

$$D_1^{ij} = \sum_{k=1}^N \int_{z_k}^{z_{k+1}} E_x^{(k)} \phi^i(z) \phi^j(z) dz$$

$$D_2^{ij} = \sum_{k=1}^N \int_{z_k}^{z_{k+1}} G_{xz}^{(k)} \frac{d\phi^i}{dz} \frac{d\phi^j}{dz} dz$$

for all $i, j = 1, 2, \dots, N$

The above presentation completes the derivation of the constitutive equations of the theory. In the following section we present the finite element formulation.

3 BLCS FINITE ELEMENT FORMULATION

The generalized displacements of the finite element are expressed in terms of nodal displacements using interpolation functions:

$$(u, w, U^j) = \sum_{i=1}^m H_i(u_i, w_i, U_i^j) \quad (8)$$

where H_i are the interpolation functions for the element, and m is the number of nodes per element. The displacement vectors in BLCS are expressed as

$$\{\Delta^0\}^T = \{u_1 w_1 \dots u_m w_m\}, \quad \{\Delta^j\} = \{U^j\}$$

where the superscript 0 refers to the value at the reference axis. Thus, the strain-displacement relation is defined as

$$\{\varepsilon^0\} = [B_L] \{\Delta^0\}, \quad \{\varepsilon^j\} = [\bar{B}_L] \{\Delta^j\} \quad (9)$$

The compatibility matrices $[B_L]$ and $[\bar{B}_L]$ expressed in terms of the interpolation functions are

$$[B_L]_{(2 \times 2m)} = \begin{bmatrix} \frac{\partial H_1}{\partial x} & 0 & \frac{\partial H_2}{\partial x} & 0 & \dots & \frac{\partial H_m}{\partial x} & 0 \\ 0 & \frac{\partial H_1}{\partial x} & 0 & \frac{\partial H_2}{\partial x} & \dots & 0 & \frac{\partial H_m}{\partial x} \end{bmatrix}$$

$$[\bar{B}_L]_{(2 \times m)} = \begin{bmatrix} \frac{\partial H_1}{\partial x} & \frac{\partial H_2}{\partial x} & \dots & \frac{\partial H_m}{\partial x} \\ H_1 & H_2 & \dots & H_m \end{bmatrix}$$

The element model can now be derived using the equilibrium condition. Based on the principle of virtual work, the equilibrium equation can be obtained from

$$\int_v \sigma \delta \varepsilon dv = \int_v f_i \delta \Delta dv + \int_s t_i \delta \Delta ds \quad (10)$$

where f_i are body forces and t_i are surface forces. Neglecting body forces, the external work done by applied forces becomes

$$\int_s t_i \delta \Delta ds = \int_0^L [f_z \delta w + f_x \delta u] dx + \sum_{j=1}^N \int_{-h/2}^{h/2} \phi^j(z) \{\delta U^j\}^T \{f_x^j\} dz = \{\delta \Delta^0\}^T \{F\} + \sum_{j=1}^N \{\delta \Delta^j\}^T \{F_x^j\} \quad (11)$$

where $\{F\}$ includes transverse (f_z) and axial (f_x) force vectors applied at the reference axis, and $\{F_x^j\}$ contains axial (f_x^j) force vectors applied at the laminate interfaces. Then, eqn (10) can be written as

$$b \int_0^L \int_{-h/2}^{h/2} \{\sigma_x \sigma_{xz}\} \begin{Bmatrix} \delta \varepsilon_x^0 + \delta \varepsilon_x^i \\ \delta \gamma_{xz}^0 + \delta \gamma_{xz}^i \end{Bmatrix} dz dx - \{\delta \Delta^0\}^T \{F\} - \sum_{j=1}^N \{\delta \Delta^j\}^T \{F_x^j\} = 0 \quad (12)$$

The virtual strains are expressed as

$$\delta \varepsilon_x^0 + \delta \varepsilon_x^i = \frac{d \delta u}{dx} + \sum_{j=1}^N \phi^j \frac{d \delta U^j}{dx}; \quad \delta \gamma_{xz}^0 + \delta \gamma_{xz}^i = \frac{d \delta w}{dx} + \sum_{j=1}^N \delta U^j \frac{d \phi^j}{dz} \quad (13)$$

Substituting eqn (13) into eqn (12) and using eqns (6), we have

$$\int_0^L [\{\delta \varepsilon^0\}^T \{N\} + \sum_{j=1}^N \{\delta \varepsilon^j\}^T \{N^j\}] dx - \{\delta \Delta^0\}^T \{F\} - \sum_{j=1}^N \{\delta \Delta^j\}^T \{F_x^j\} = 0 \quad (14)$$

where

$$\{\delta \varepsilon^0\} = \begin{Bmatrix} \frac{d \delta u}{dx} \\ \frac{d \delta w}{dx} \end{Bmatrix}, \quad \{\delta \varepsilon^j\} = \begin{Bmatrix} \frac{d \delta U^j}{dx} \\ \delta U^j \end{Bmatrix}, \quad \{N\} = \begin{Bmatrix} N_x \\ N_{xz} \end{Bmatrix}, \quad \{N^j\} = \begin{Bmatrix} N_x^j \\ N_{xz}^j \end{Bmatrix}$$

and from eqn (7) and eqn (9), the resultant force vectors are

$$\begin{aligned} \{N\} &= b[A][B_L]\{\Delta^0\} + b \sum_{j=1}^N [B^j][\bar{B}_L]\{\Delta^j\} \\ \{N^j\} &= b[B^j][\bar{B}_L]\{\Delta^0\} + b \sum_{k=1}^N [D^{jk}][\bar{B}_L]\{\Delta^k\} \end{aligned} \quad (15)$$

By substituting eqn (15) and the virtual strain vectors from eqn (9) into eqn (14), we have

$$\begin{aligned} &\{\delta \Delta^0\}^T \left[\int_0^L [B_L]^T [A][B_L]\{\Delta^0\} + \sum_{j=1}^N [B_L]^T [B^j][\bar{B}_L]\{\Delta^j\} dx - \frac{1}{b} \{F\} \right] \\ &+ \sum_{j=1}^N \{\delta \Delta^j\}^T \left[\int_0^L [\bar{B}_L]^T [B^j][\bar{B}_L]\{\Delta^0\} + \sum_{k=1}^N [\bar{B}_L]^T [D^{jk}][\bar{B}_L]\{\Delta^k\} dx - \frac{1}{b} \{F_x^j\} \right] = 0 \end{aligned} \quad (16)$$

Expanding the summations in eqn (16), we obtain N simultaneous equations for the element model as follows:

$$\begin{bmatrix} [A_1] & [B_1] & [B_2] & \dots & [B_N] \\ [B_1]^T & [D_{11}] & [D_{12}] & \dots & [D_{1N}] \\ \vdots & \vdots & \vdots & \ddots & \vdots \\ [B_N]^T & [D_{N1}] & [D_{N2}] & \dots & [D_{NN}] \end{bmatrix} \begin{Bmatrix} \{\Delta^0\} \\ \{\Delta^1\} \\ \vdots \\ \{\Delta^N\} \end{Bmatrix} = \frac{1}{b} \begin{Bmatrix} \{F\} \\ \{F_x^1\} \\ \vdots \\ \{F_x^N\} \end{Bmatrix} \quad (17)$$

where

$$[A_1] = \int_0^L [B_L]^T [A][B_L] dx$$

$$[B_i] = \int_0^L [B_L]^T [B^i] [\bar{B}_L] dx$$

$$[D_{ij}] = \int_0^L [\bar{B}_L]^T [D^{ij}] [\bar{B}_L] dx$$

The dimensions of $[A_1]$, $[B_i]$ and $[D_{ij}]$ are $(2m \times 2m)$, $(2m \times m)$, and $(m \times m)$ respectively. Therefore, the total degrees of freedom per element are $2m + mN$. The layer-wise constant shear stresses are transformed into parabolic distributions, as discussed next.

4 COMPUTATION OF PARABOLIC SHEAR STRESS

Based on the suggestions given by Chaudhuri and Seide²⁰ and Reddy *et al.*,⁹ the layer-wise constant shear stresses are transformed into parabolic distributions. The stresses at the i th layer are obtained from constitutive relations:

$$\sigma_x^{(i)} = E_x^{(i)} \epsilon_x^{(i)}, \quad \sigma_{xz}^{(i)} = G_{xz}^{(i)} \gamma_{xz}^{(i)} \quad (18)$$

The constant shear stress σ_{xz} in the i th layer is interpolated using quadratic functions to obtain a parabolic distribution as follows:

$$\sigma_{xz}^{(i)}(\bar{z}) = \sum_{j=1}^3 \phi_j(\bar{z}) \sigma_j^{(i)} \quad (19)$$

where \bar{z} is a non-dimensional local coordinate with the origin at the bottom surface of the i th layer; $\sigma_1^{(i)}$, $\sigma_2^{(i)}$, and $\sigma_3^{(i)}$ are, respectively, the shear stresses at the bottom, middle and top of the i th layer, and ϕ_j are the second order Lagrangian polynomials. The Lagrangian polynomials $\phi_j(\bar{z})$ can be expressed in terms of a global coordinate z with origin at the midsurface of the beam:

$$\phi_1(z) = 1 - 3 \frac{(z - z_i)}{h^i} + 2 \left(\frac{z - z_i}{h^i} \right)^2$$

$$\phi_2(z) = 4 \frac{(z - z_i)}{h^i} - 4 \left(\frac{z - z_i}{h^i} \right)^2$$

$$\phi_3(z) = -\frac{(z - z_i)}{h^i} + 2 \left(\frac{z - z_i}{h^i} \right)^2$$

where $h^i = z_{i+1} - z_i$ is the thickness of the i th layer. For a laminated beam with N layers, $3N$ equations are necessary to obtain layer-wise parabolic shear stress distributions through the cross-section. The required number of equations can be derived from the following four conditions: (1) N equations are used to equate the average shear stress with the constant shear stress from constitutive equation on each layer; (2) two equations are used to impose zero-shear condition at the surfaces of the beam; (3) $N - 1$ equations are used to satisfy continuity of shear stresses at the interfaces; and (4) $N - 1$ equations are used to define the slope discontinuities $\sigma_{xz,z}$ at each interface. Using eqn (19), the condition (1) yields

$$\frac{1}{h^i} \int_{z_i}^{z_{i+1}} \sum_{j=1}^3 \phi_j(z) \sigma_j^{(i)} dz = \frac{1}{6} [\sigma_1^{(i)} + 4\sigma_2^{(i)} + \sigma_3^{(i)}] = \sigma_{xz}^{(i)} \quad (20)$$

The shear-free conditions on the top and bottom surfaces of the beam are

$$\sigma_1^{(1)} = \sigma_3^{(N)} = 0 \quad (21)$$

At the interfaces shear stresses satisfy the continuity condition

$$\sigma_3^{(i)} - \sigma_1^{(i+1)} = 0 \quad (22)$$

Finally, the slope discontinuity of the shear stress at an interface becomes

$$\sigma_{xz,z}^{(i+1)} - \sigma_{xz,z}^{(i)} = \frac{1}{h^i} (-\sigma_1^{(i)} + 4\sigma_2^{(i)} - 3\sigma_3^{(i)}) + \frac{1}{h^{i+1}} (-3\sigma_1^{(i+1)} + 4\sigma_2^{(i+1)} - \sigma_3^{(i+1)}) \quad (23)$$

To satisfy stress equilibrium, the variation of the shear stress can be equated to the variation of the normal stress as

$$\sigma_{xz,z} = -\sigma_{xx,x} \quad (24)$$

The evaluation of $\sigma_{xx,x}$ requires the second derivatives of u and U^j :

$$\sigma_{xx,x} = E_x \varepsilon_{x,x} = E_x \left[\frac{d^2 u}{dx^2} + \sum_{j=1}^N \frac{d^2 U^j}{dx^2} \phi^j(z) \right]$$

where the second derivatives of the displacements for an m -node element are

$$\frac{d^2 u}{dx^2} = \sum_{i=1}^m u_i \frac{d^2 H_i}{dx^2}, \quad \frac{d^2 U^j}{dx^2} = \sum_{i=1}^m U_i^j \frac{d^2 H_i}{dx^2}$$

and the second derivatives of the interpolation functions H_i are calculated as

$$\frac{d^2 H_i}{dx^2} = \frac{1}{J^2} \frac{d^2 H_i}{d\xi^2} - \frac{1}{J^3} \frac{dH_i}{d\xi} \sum_{k=1}^m x_k \frac{d^2 H_k}{d\xi^2}$$

where J is the Jacobian. By arranging eqns (20)–(24) with respect to unknowns $\sigma_j^{(i)}$, we obtain $3N$ simultaneous equations, whose solution gives a parabolic distribution of shear stress through the thickness.

5 NUMERICAL EXAMPLES

To assess the capability of the model and its accuracy, various examples are solved and the results are compared with available solutions. A three-node BLCS finite element integrated with two Gauss points along the element axis is used. The stresses evaluated at the Gauss points are extrapolated to the nodes using linear interpolation functions, as suggested by Cook *et al.*²⁴

Example 1: effect of shear deflection

The maximum deflection for a simply supported isotropic beam, subjected to a uniform load, is computed with BLCS for various width-to-span ratios (H/L). The results are compared with elasticity and numerical solutions used previously by Yuan and Miller.²¹ The maximum deflection ratio, defined as deflection including shear effects to deflection computed from Bernoulli–Euler beam theory, is shown in Table 1. The results presented with BLCS used four elements with four layers.

Table 1. Maximum deflection ratio

| H/L | 1.0 | 0.8 | 0.6 | 0.4 | 0.2 | 0.1 |
|--|------|------|------|------|------|------|
| Timoshenko and Goodier ²⁵ (2-D elasticity) | 3.28 | 2.46 | 1.82 | 1.36 | 1.09 | 1.02 |
| Rehfield and Murthy ³ | 3.28 | 2.46 | 1.82 | 1.36 | 1.09 | 1.02 |
| Yuan and Miller ²¹ (8 elements; 3 layers) | 3.25 | 2.45 | 1.82 | 1.36 | 1.09 | 1.02 |
| Levinson ² | 3.49 | 2.60 | 1.90 | 1.40 | 1.10 | 1.02 |
| BLCS (4 elements; 4 layers) | 3.33 | 2.50 | 1.85 | 1.38 | 1.09 | 1.02 |

When compared to the elasticity solution (Timoshenko & Goodier²⁵), the BLCS results are about 2% higher for $H/L = 1.0$. As discussed by Levinson,² the reason for this discrepancy is the transverse incompressibility assumption used in the formulation.

Example 2: stress and displacement ratios

The stress and displacement ratios of a fixed-fixed sandwich beam under an uniform load (Fig. 2) are compared with other studies. The stress ratio (SR)

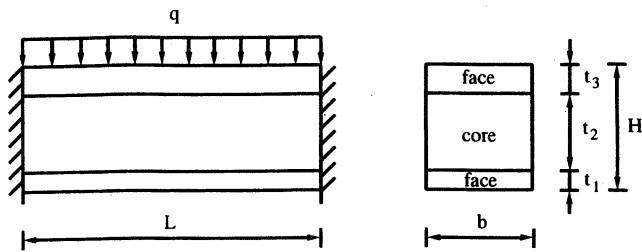


Fig. 2. Fixed-fixed sandwich beam with uniform load.

Table 2. Material and thickness combination

| Case | E_2/E_1 | t_3/t_1 | t_2/t_1 |
|------|-----------|-----------|-----------|
| A | 0.2 | 10 | 10 |
| B | 0.1 | 10 | 20 |
| C | 0.01 | 10 | 20 |
| D | 0.2 | 0.5 | 1 |

Note: $E_2/G_2 = 2.5$, $E_3/E_1 = 1$ for all cases.

is defined as the maximum normal stress at the midspan of the beam divided by the maximum stress in an isotropic beam made of the face material and analyzed by classical beam theory. The displacement ratio (DR) is the ratio of the maximum deflection in the sandwich beam to that of an isotropic beam made of the face material. The face and core material and thickness combination are given in Table 2. DiTaranto²⁶ neglected the bending stiffness of the core and the shear deformation of the faces. Realizing the significance of the bending stiffness of the core in a stiff-cored or thick-cored or highly unsymmetric sandwich beam, Rao²⁷ included the bending stiffness of the core but neglected the shear deformation of the faces. In BLCS, to include the shear deformation of the faces, the shear modulus of the face material is assumed to be equal to $0.4E_1$ (or 0.25 for Poisson's ratio). One half of the sandwich beam is analyzed with eight elements, each having six layers. As shown in Table 3, the BLCS predictions compared reasonably well with those of others, especially with Yuan and Miller's values. However, Yuan and Miller did not report the shear moduli of the faces.

Example 3: experimental-BLCS stress comparisons

Using photoelasticity, Kemmochi and Uemura²⁸ measured the stress distribution in four three-layered beams, which were tested in bending under symmetric two-point loading, as shown in Fig. 3. The material properties of the three types

Table 3. Displacement and stress ratios

| Case | DiTaranto | | Rao | | Yuan & Miller | | BLCS | |
|------|-----------|-------------------|------|-------------------|---------------|------|------|------|
| | DR | SR | DR | SR | DR | SR | DR | SR |
| A | 3.16 | — | 2.45 | — | 2.82 | 2.06 | 2.83 | 2.08 |
| B | 6.25 | 5.41 | 4.95 | 3.26 | 5.09 | 3.21 | 5.07 | 3.23 |
| C | 16.1 | 3.65 | 15.9 | 3.35 | 16.7 | 3.37 | 16.7 | 3.41 |
| D | 2.30 | 1.40 ^a | 2.30 | 1.40 ^a | 2.46 | 1.23 | 2.49 | 1.33 |

^aValues obtained from Rao,²⁷ Fig. 9, p. 395, which do not coincide with values reported by Yuan and Miller,²¹ Table 2, p. 744.

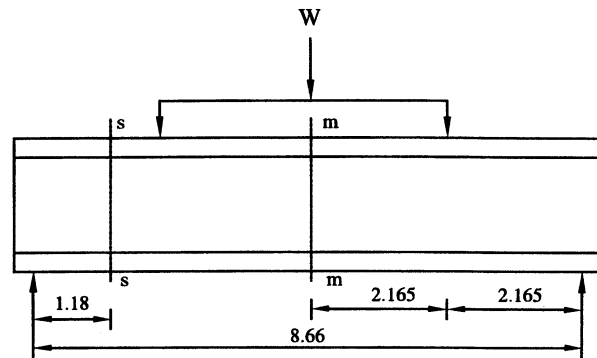


Fig. 3. Sandwich beam under two-point bending (units: lb and in).

Table 4. Laminae material properties

| | A | B | C |
|-------------------|------------|------------|--------------|
| E , (MPa) (ksi) | 2440 (354) | 521 (75.5) | 4.34 (0.629) |
| G , (MPa) (ksi) | 875 (127) | 181 (26.2) | 1.53 (0.222) |

of laminae used are given in Table 4, and the material and thickness combinations of the core and face layers for the four beams are given in Table 5. Kemmochi and Uemura predicted the response of the test-beams by a multi-layer built-up theory. In BLCS, 16 elements with eight layers are used to compute the stresses at sections s-s (constant shear) and m-m (maximum moment). In the figures reported by Kemmochi and Uemura²⁸ it appears that the labels for transverse normal and shear stresses are switched. In Fig. 4, the BLCS and experimental normal and shear stress distributions are compared at section s-s, and in Fig. 5, the BLCS and multi-layer built-up theory normal stress predictions are compared to experimental measurements at section m-m. The BLCS predictions agree closely with the experimental results. The BLCS accuracy for predicting the stress is particularly significant in model 4, which

Table 5. Test model specification

| | Material face/core | Thickness, mm (in) | | Width, mm (in) | Load (W), N (lb) |
|---------|--------------------|--------------------|-------------|---------------------------|------------------|
| | | Face | Core | | |
| Model 1 | A/A | 4.48 (0.176) | 30.0 (1.18) | 6.56 (0.258) | 98 (22.03) |
| Model 2 | A/B | 4.76 (0.187) | 30.0 (1.18) | 6.57 (0.259) ^a | 98 (22.03) |
| Model 3 | B/C | 4.51 (0.178) | 30.0 (1.18) | 6.32 (0.249) | 9.8 (2.203) |
| Model 4 | A/C | 4.72 (0.186) | 30.0 (1.18) | 6.57 (0.259) ^a | 9.8 (2.203) |

^aIn the experiment, the face width was a little larger than that of the core. The face width is used for core and face in BLCS.

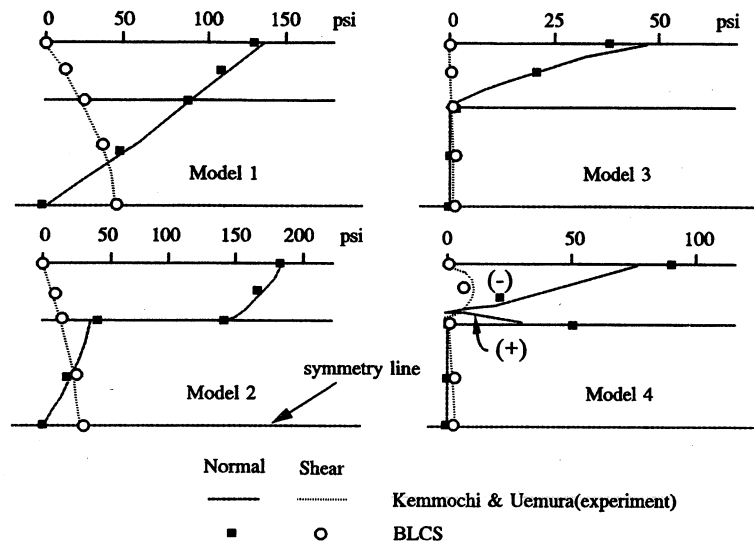


Fig. 4. Stress distribution at section s-s.

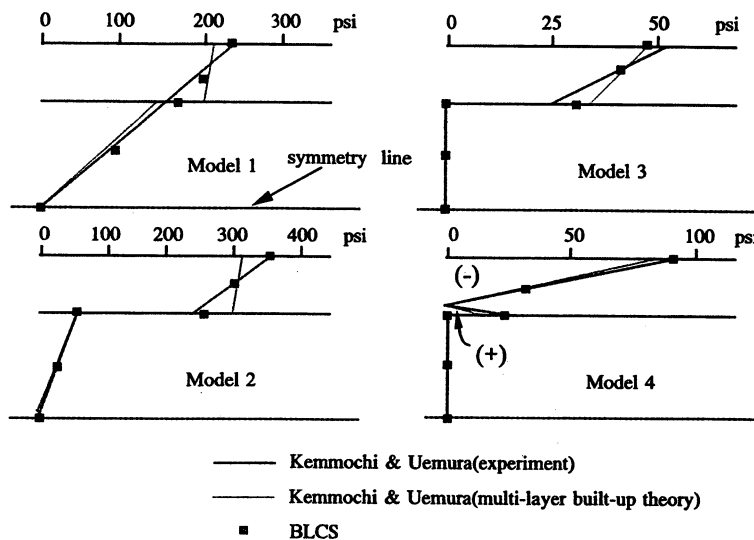


Fig. 5. Normal stress distribution at section m-m.

has a very low core stiffness compared to face stiffness.

Example 4: elasticity-BLCS comparisons

Cheng *et al.*⁵ derived a 3-D elasticity solution for unidirectionally reinforced and symmetric lami-

nated beams. The solution was illustrated for a three-layered cantilever beam under a tip load (Fig. 6). The following material properties and geometric parameters are used: $E_1 = 1.04 \times 10^6$ kg/cm², $G_1 = 4 \times 10^5$ kg/cm², $E_2 = 2.08 \times 10^6$ kg/cm², $G_2 = 8 \times 10^5$ kg/cm², $\nu = 0.3$, $a_1 = 5$ cm, $a = 15$ cm, $b = 10$ cm, and $L = 75$ cm. In the BLCS

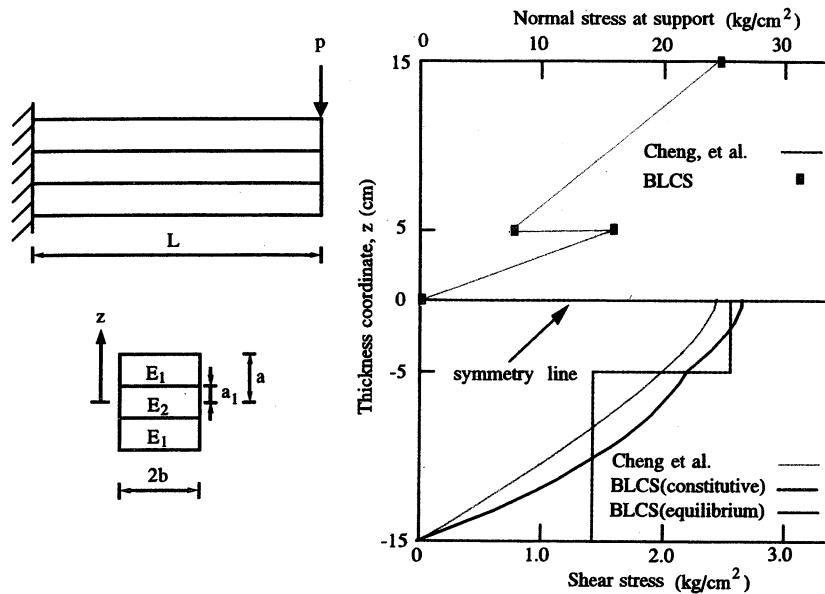


Fig. 6. Cantilever under concentrated tip load and stress distribution.

analysis, one element with four layers is used. The normal stress distribution of BLCS at the support is very close to the elasticity result, but there is a little difference in shear stress distribution (Fig. 6). The difference is mainly due to the 3-D effect included in the elasticity solution and the different boundary conditions imposed at the support, i.e. the longitudinal displacement in BLCS is fixed through the thickness, whereas in the elasticity solution, it is fixed only at the center of the section.

Example 5: displacement, shear and normal stress comparisons

A symmetrically laminated cantilever beam is analyzed for two load cases: a uniformly distributed load, and a concentrated tip load (Fig. 7). The laminate material properties and loading cases are given in Table 6. Surana and Nguyen¹⁵ analyzed this problem using nine, 2-D curved beam finite elements, derived by approximating the transverse displacement with a polynomial of variable order p . In the BLCS analysis, eight elements with eight layers are used. The displacements are compared in Table 7, and the stresses are compared in Figs 8 and 9. The BLCS results agree very well with Surana and Nguyen's solution, which used a 16th order polynomial approximation ($p=16$) for the transverse direction.

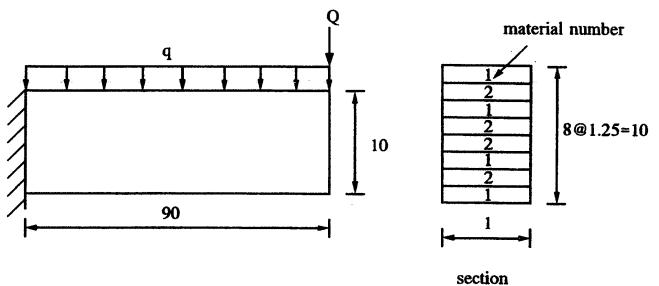


Fig. 7. Beam configuration and section.

6 SUMMARY AND CONCLUSION

A three-node, laminated beam finite element with layer-wise constant shear (BLCS) is formulated using a two-Gauss-point quadrature rule along the element axis and assuming transverse incompressibility and layer-wise linear distribution of in-plane displacement. The constitutive equation for a lamina is based on plane stress, both through the thickness and width of the beam. The laminate constitutive equations are calculated using the constitutive equations and linear interpolation functions of in-plane displacement of the laminae. Using the principle of virtual work, the element stiffness matrix is derived, which has $2 + N$ degrees of freedom per node of an N -layer beam. The deformed cross-section is not plane through the thickness but plane on each layer. The layer-wise constant shear distribution obtained from

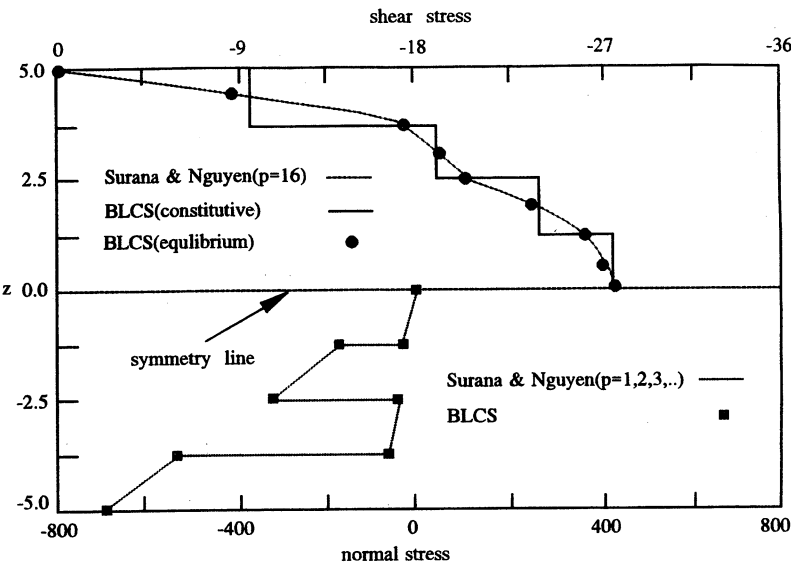


Fig. 8. Stresses at $X = L/2$ (case A).

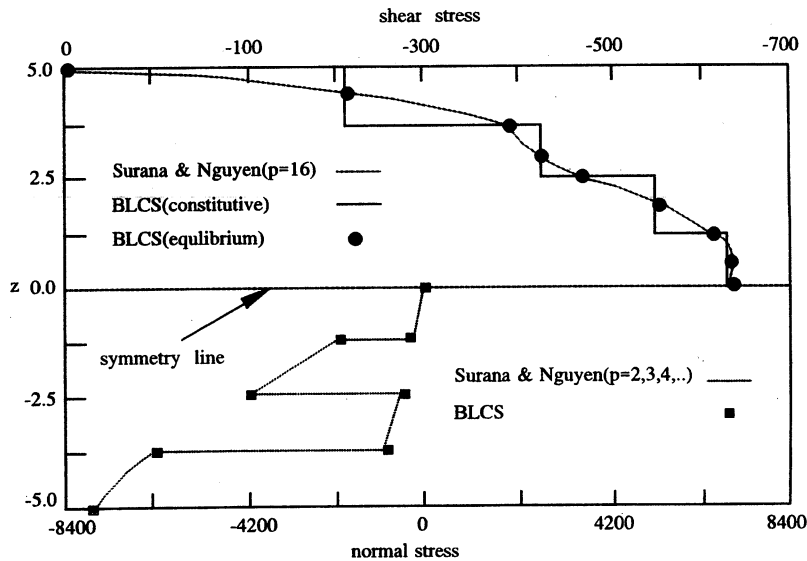


Fig. 9. Stresses at $X = L/2$ (case B).

Table 6. Material properties and loading case

| Material | | Loading case | |
|-------------------------|-------------------------|--------------|-----------|
| Material 1 | Material 2 | Case A | Case B |
| $E_x/E_y = 30$ | $E_x/E_y = 5$ | | |
| $E_y = 1.0 \times 10^6$ | $E_y = 1.0 \times 10^6$ | $Q = 200$ | $Q = 0$ |
| $G_{xy}/E_y = 0.5$ | $G_{xy}/E_y = 0.5$ | $q = 0$ | $q = 100$ |
| $\nu_{xy} = 0.25$ | $\nu_{xy} = 0.25$ | | |

Table 7. Maximum deflection

| | Case A | Case B |
|---|---------|--------|
| Surana and Nguyen ¹⁵ ($p = 16$) | 0.03031 | 0.535 |
| BLCS | 0.03029 | 0.552 |

constitutive relations is modified into a parabolic distribution by using compatibility and equilibrium of the shear stress at each layer. Several experimental and numerical examples available in the literature are used to evaluate the accuracy of the BLCS element. Compared with the results of other studies, the prediction of the displacements and stresses of the BLCS element are quite accurate. The examples presented in this paper show that the BLCS element can be used for the accurate analysis of sandwich beams with soft cores. Furthermore, the simplicity of the element makes it suitable for the analysis of frame-type structures.

REFERENCES

1. Rao, K. M. & Ghosh, B. G., Exact analysis of unsymmetric laminated beam. *J. Struct. Div., ASCE*, **105** (11) (1979) 2313–25.
2. Levinson, M., A new rectangular beam theory. *J. Sound Vib.*, **74** (1) (1981) 81–7.
3. Rehfield, L. W. & Murthy, P. L. N., Toward a new engineering theory of bending: fundamentals. *AIAA J.*, **20** (5) (1982) 693–9.
4. Krishna Murty, A. V., Toward a consistent beam theory. *AIAA J.*, **22** (6) (1984) 811–16.
5. Cheng, S., Wei, X. & Jiang, T., Stress distribution and deformation of adhesive-bonded laminated composite beams. *J. Engng Mech.*, **115** (6) (1989) 1150–62.
6. Timoshenko, S. P., *History of Strength of Materials*. McGraw-Hill, New York, 1953.
7. Reddy, J. N., A simple higher-order theory for laminated composite plates. *J. Appl. Mech.*, **51** (1984) 745–52.
8. Reddy, J. N., A generalization of two-dimensional theories of laminated composite plates. *Commun. Appl. Numer. Meth.*, **3** (1987) 173–80.
9. Reddy, J. N., Barbero, E. J. & Teply, J. L., A plate bending element based on a generalized laminate plate theory. *Int. J. Numer. Meth. Engng*, **28** (1989) 2275–92.
10. Kant, T. & Gupta, A., A finite element model for a higher-order shear-deformable beam theory. *J. Sound Vib.*, **125** (2) (1988) 193–202.
11. Kant, T. & Manjunath, B. S., Refined theories for composite and sandwich beams with C^0 finite elements. *Comput. Struct.*, **33** (3) (1989) 755–64.
12. Gordaninejad, F. & Ghazavi, A., Effect of shear deformation on bending laminated composite beams. *J. Press. Vess. Technol.*, **111** (1989) 159–64.
13. Yuan, F. G. & Miller, R. E., Higher-order finite element for short beams. *AIAA J.*, **26** (11) (1988) 1415–17.
14. Yuan, F. G. & Miller, R. E., A higher order finite element for laminate beams. *Comp. Struct.*, **14** (1990) 125–50.
15. Surana, K. S. & Nguyen, S. H., Two-dimensional curved beam element with higher-order hierarchical transverse approximation for laminated composites. *Comp. Struct.*, **36** (3) (1990) 499–511.
16. Noor, A. K. & Burton, W. S., Assessment of shear deformation theories for multilayered composite plates. *Appl. Mech. Rev.*, **42** (2) (1989) 1–13.
17. Kapania, R. K. & Raciti, S., Recent advances in analysis of laminated beams and plates, Part 1: Shear effect and buckling. *AIAA J.*, **27** (7) (1989) 923–34.
18. Kassapoglou, C. & Lagace, P. A., An efficient method for the calculation of interlaminar stresses in composite materials. *J. App. Mech.*, **53** (1986) 744–50.
19. Lajczok, M. R., New approach in the determination of interlaminar shear stresses from the results of MSC/NASTRAN. *Comput. Struct.*, **24** (4) (1986) 651–6.
20. Chaudhuri, R. A. & Seide, P., An approximate semi-analytical method for prediction of interlaminar shear stresses in an arbitrarily laminated thick plate. *Comput. Struct.*, **25** (4) (1987) 627–36.
21. Yuan, F. G. & Miller, R. E., A new finite element for laminated composite beams. *Comput. Struct.*, **31** (5) (1989) 737–45.
22. Barbero, E. J., On a generalized laminate theory with application to bending, vibration, and delamination buckling in composite laminates. PhD dissertation, Department of Engineering Mechanics, VPI & SU, Blacksburg, VA, 1989.
23. Jones, R. M., *Mechanics of Composite Materials*. McGraw-Hill, New York, 1975.
24. Cook, R. D., Malkus, D. S. & Plesha, M. E., *Concepts and Applications of Finite Element Analysis*, 3rd edn. John Wiley, New York, 1989.
25. Timoshenko, S. P. & Goodier, J. N., *Theory of Elasticity*, 3rd edn. McGraw-Hill, New York, 1970.
26. DiTaranto, R. A., Static analysis of a laminated beam. *J. Engng Ind.*, **95** (1973) 755–61.
27. Rao, D. K., Static response of stiff-cored unsymmetric sandwich beams. *J. Engng Ind.*, **98** (1976) 391–6.
28. Kemmochi, K. & Uemura, M., Measurement of stress distribution in sandwich beams under four-point bending. *Exper. Mech.*, **20** (1980) 80–6.

